Xinyu Shen, Bo Li, Yung-Tsang Chen, Walid Tizani, Yi Jiang, 2022, Relocating plastic hinges in reinforced concrete beam-column joints by mechanically anchored diagonal bars, Engineering Structures, Volume 251, Part A, 2022, 113468, ISSN 0141-0296, https://doi.org/10.1016/j.engstruct.2021.113468.

Relocating plastic hinges in reinforced concrete beam-column joints by mechanically anchored diagonal bars

Xinyu Shen[1], Bo Li[1,*] Yung-Tsang Chen[1], Walid Tizani[2], Yi Jiang[3]

[1] Department of Civil Engineering, University of Nottingham Ningbo China, Ningbo 315100, China

[2] Department of Civil Engineering, University of Nottingham, Nottingham NG7 2RD, UK

[3] Ningbo Construction Engineering Group Co., LTD, Ningbo 315100, China

[*]Corresponding author: bo.li@nottingham.edu.cn

Abstract

The implementation of strong column-weak beam concept in reinforced concrete (RC) moment-resisting frames results in the formation of plastic hinges at the beam ends, which could lead to the strain penetration of beam longitudinal reinforcement into beam-column joint (BCJ) cores. This causes high shear forces inside joint cores, bonding deterioration of longitudinal reinforcement and consequently jeopardizes the seismic behaviour of BCJs. Plastic hinge relocation by mechanically anchored diagonal bars has been proposed to mitigate such potential damage to BCJ cores. This paper investigates the effect of relocating distance of plastic hinge on the seismic performance of BCJs with mechanically anchored diagonal bars. Five interior BCJ specimens including one control specimen reinforced with conventional stirrups and four others reinforced with mechanically anchored diagonal bars were tested under cyclic load. Test results indicate that the plastic hinges can be generally relocated by different distances to the anchorage ends of diagonal bars. Increasing the relocating distance can enhance the loading capacity and stiffness of BCJs, but also increase the potential of joint shear failure. The ductility, energy dissipation and joint shear deformation of BCJs are first improved then reduced as the relocating distance increases. Although the strain penetration of beam longitudinal reinforcement into the joint cores can be gradually alleviated as the plastic hinges

are moved farther away from the joints, the induced bending moments at the beam ends are amplified and subsequently increase the joint shear forces. Moreover, increasing the length of anchorage segments increases the forces sustained by the mechanically anchored diagonal bars. Therefore, a lower bound of the relocating distance of plastic hinges is recommended to take advantage of the benefits from reduced strain penetration, while an upper limit needs to be specified to avoid joint shear failure. In addition, an analytical model is developed to predict the failure modes and loading capacities of BCJs with the plastic hinges relocated by different distances. A satisfactory agreement between the prediction and the experimental results is obtained.

Keywords: Beam-column joints; joint reinforcement; plastic hinge relocation; mechanical anchorage; diagonal bars; seismic performance.

1. Introduction

Beam-column joints (BCJs) play an important role in transferring loads between beams and columns in the moment-resisting frame structures. During an earthquake, the shear force inside BCJs is much higher than that in their adjacent elements due to the opposite bending moments across the joint cores [1]. Without proper detailing, the deformation of BCJs can contribute to more than 60% of the story drift [2]. Furthermore, once the brittle shear failure occurs inside joint cores, the BCJs lose their integrity and act as hinges, leading to the collapse of buildings [3,4]. Therefore, the BCJs have to be adequately designed to avoid their failure before adjacent beams and columns. Meanwhile, the "strong column-weak beam" concept is commonly adopted in the codes [5–7] for frame structures to ensure their energy dissipation, ductility [8] and uniform inter-storey drift along the height [9]. Nevertheless, when plastic hinges form at the beam ends, the yielding of beam longitudinal reinforcement at the beam-joint interfaces results in a significant joint shear force. It is also inevitable that the yielding strains of beam longitudinal reinforcement at the beam-joint interfaces would penetrate into the joint cores and deteriorate bonding condition of longitudinal reinforcement with joint concrete [10,11]. This could lead to cracking and damage of BCJ cores, which are usually difficult to retrofit [12]. Therefore, a certain amount of horizontal stirrups is required inside the joint cores to ensure the strength of BCJs in accordance with conventional design philosophies [1]. However, the conventional shear reinforcement is detrimental to the construction efficiency and productivity due to the problem of reinforcement congestion inside joint cores [13]. Alternative solutions are needed to improve the constructability of BCJs without compromising their seismic behaviour.

To reduce the amount of joint stirrups and improve the seismic performance of BCJs, the authors of this study proposed a novel joint reinforcement detail in a previous study [14]. The proposed detail is in the form of unbonded diagonal bars with anchorage segments in beams.

Compared to conventional stirrups, the proposed detail is able to improve the seismic performance of BCJs by means of plastic hinge relocation and force self-balancing mechanisms. It can also reduce the amount of joint stirrups to 1/3 of that specified in the local code [5]. Among the two mechanisms, the plastic hinge relocation aims at improving the bonding condition of beam longitudinal reinforcement by providing longer development length and protecting the joint core by reducing yielding penetration. The plastic hinge relocation was realized by the anchorage segments that enhanced the flexural capacity of beam ends. However, the anchorage length was merely controlled at $0.5h_b$ in all the tested specimens in the previous study, leading to the plastic hinges relocated by the same distance. Thus, the influence of the anchorage length on the effectiveness of the proposed reinforcement detail and seismic performance of BCJs needs to be further studied.

Despite that the plastic hinge relocation has been widely studied for both new constructed BCJs [15–20] and retrofitted BCJs [21–27], there are limited studies focusing on the effect of relocating distance of plastic hinges on the performance of BCJs. Park and Milburn [15] used additional straight bars with 90° hooks to relocate beam plastic hinges for both exterior and interior BCJs. The additional bars were anchored in beams by a length of $1.1h_b$ with h_b being the height of beam cross-section. Although the plastic hinges were relocated, the BCJs still failed by joint shear at the late loading stage. Sharif and Ketabi [16] also used straight bars with 90° hooks to relocate plastic hinges for exterior BCJs. It was found that the BCJs with additional straight bars anchored in beam for a length of h_b failed by relocated plastic hinges without triggering joint shear failure. Hwang et al. [17] reported that the plastic hinges in BCJs were relocated by $0.42h_b$ and $0.6h_b$ when the additional straight bars were anchored with 45° bent and 90° hook, respectively. However, the BCJ with plastic hinges relocated by $0.6h_b$ showed significant diagonal cracks in the joint core. Chutarat and Aboutaha [18] successfully relocated the plastic hinges to the anchorage ends of additional straight headed bars installed

in exterior BCJs. The authors also stated that the plastic hinge relocation increased the joint shear force. Galunic et al. [19] relocated the plastic hinges in BCJs by $1.33h_b$ and $1.5h_b$ through installing additional 60° bent bars and straight bars, respectively. The authors found that the bonding condition of longitudinal bars was improved and the BCJ specimens showed little damage inside the joint cores. Eom et al. [20] installed straight bars with anchorage heads or 90° hook to improve bonding condition of beam longitudinal bars for interior BCJs. The anchorage length of the bars in beams was controlled at $0.5h_b$. In both cases, the specimens failed by relocated plastic hinges with significantly reduced joint damage as compared to the control specimen. While the loading capacities were comparable for both specimens, the specimen with plastic hinge relocated by $0.67h_b$ exhibited fewer cracks at the joint core and the beam-joint interface than that with plastic hinge relocated by $1.0h_b$. In addition, Arowojolu *et al.* [28] relocated plastic hinges in BCJs through externally bonding CFRP sheets on beam flanges with lengths of $0.67h_b$ and $1.0h_b$, and reported that increasing the relocating distance from $0.67h_b$ to $1.0h_b$ resulted in more severe joint damage but comparable loading capacity. In general, the plastic hinge in BCJs can be relocated by different distances, depending on the details of adopted reinforcement. Although the NZS 3101 [7] specifies that the relocating distance should be larger than the beam cross-section height h_b, the above-mentioned studies indicated that plastic hinge relocation could still be achieved with a satisfactory performance of BCJs, even though the designed relocating distance is smaller than h_b. In addition, it can be found that most of the existing studies focus on verifying its effectiveness of plastic hinge relocation in improving the performance of BCJs. The influence of relocating distance of plastic hinges on the performance of BCJs remains unclear.

This paper investigates the seismic performance of BCJs reinforced with mechanically anchored diagonal bars with different lengths of anchorage segments. Five interior BCJ specimens including one control specimen reinforced by conventional stirrups and four others

reinforced by the proposed reinforcement detail were prepared and tested under cyclic loading. Their seismic performance in terms of cracking behaviour, failure mode, hysteretic characteristics, joint shear deformation, and reinforcement strain are presented. Based on the results, the effect of relocating distance of plastic hinges on the seismic performance of BCJ specimens is analysed. The influence of the anchorage length on the effectiveness of the proposed reinforcement detail is also discussed. Finally, an analytical method based on sectional analysis is developed to predict the failure modes and loading capacities of BCJs with the plastic hinges relocated by different distances.

2. Novel joint reinforcement detail

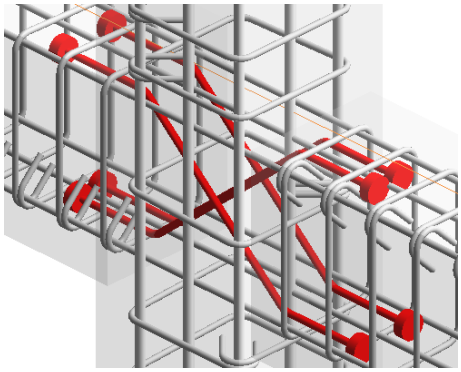

(a) Proposed joint reinforcement

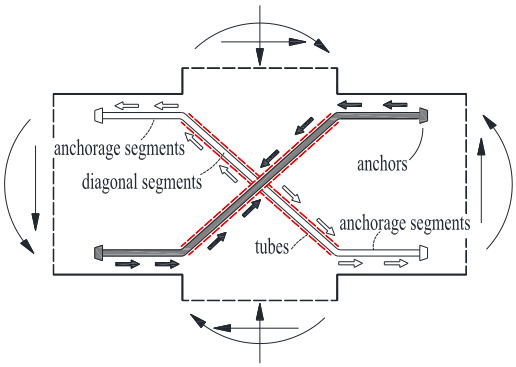

(b) Force flow on the diagonal bars

(c) Plastic tube

(d) Anchorage end

(e) Threaded end

(f) Steel anchors

Figure 1: Novel reinforcement detail for BCJs.

Figure 1 shows the novel reinforcement detail for RC interior BCJs proposed in a previous study by the authors [14]. It has been proved that the proposed reinforcement detail is able to reduce the amount of joint stirrups without compromising the performance of BCJs. As shown

in Figure 1(a), this detail is composed of steel bars placed in pairs in the joint regions. Each steel bar consists of one diagonal segment and two anchorage segments. The diagonal segments are located inside the joint core and wrapped with plastic tubes as shown in Figure 1(c). The anchorage segments are positioned parallel to the beam longitudinal reinforcement, and their ends are threaded and installed with steel anchors as shown in Figure 1(d)-1(f). The proposed novel reinforcement detail can be installed in one-way frames (e.g. factories) or the weak direction of BCJs with transverse beams. Here, the weak direction is defined as the direction with a higher joint shear force. In this case, additional J-hoops can be provided in the other direction to ensure its joint shear strength.

The plastic hinge relocation mechanism is first considered for the proposed reinforcement detail. The addition of the anchorage segments can enhance the flexural capacities of sections at beam ends. Consequently, there is a drop of flexural capacity at the ends of the anchorage segments, and the plastic hinges are expected to shift from the beam-joint interfaces to the anchorage ends. The steel anchors installed on the anchorage segments can enhance the anchorage for the diagonal segments and control the position of plastic hinges. Moreover, the proposed reinforcement detail also considers the force self-balancing mechanism through the diagonal segments, as shown in Figure 1(b). The plastic tubes wrapped on the diagonal segments aim to eliminate their bond with joint concrete. Under the horizontal load, the bending moments applied on the beam ends across a joint are in the opposite sign. Consequently, the forces on the anchorage segments at diagonally opposite sides (e.g. upper left and lower right) are both under tension or compression, and will be further transmitted to the diagonal segments. As the diagonal segments are isolated from concrete by the plastic tubes, the forces on the diagonal segments will be self-balanced without transferring to the joint concrete. In other words, the forces acting on the anchorage segments of the novel reinforcement detail would not cause shear forces in the joint core.

3. Experimental programme

3.1 Specimen description

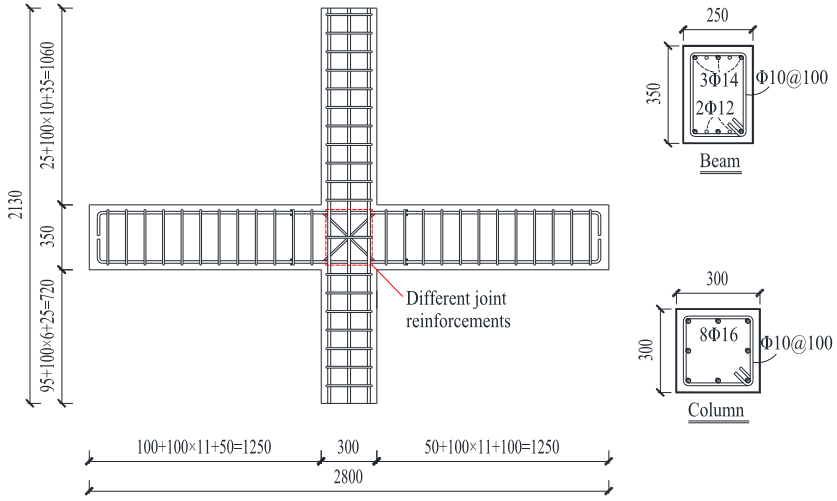

(a) Geometry, beam reinforcement and column reinforcement

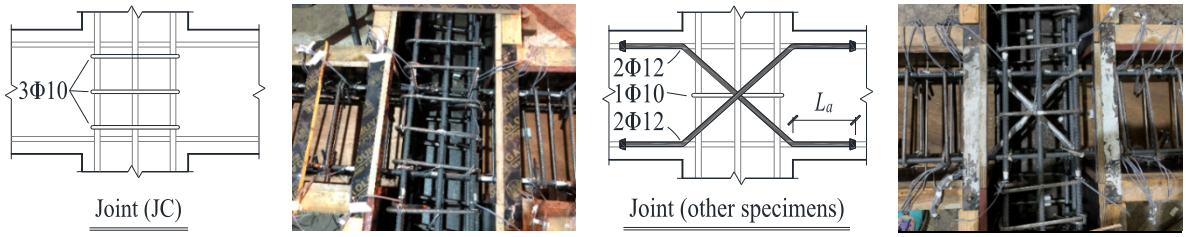

(b) Joint reinforcement

Figure 2: Dimension and reinforcement details of BCJ specimens.

Five 2/3-scale interior BCJ specimens having the same geometry, beam reinforcement and column reinforcement (Figure 2) were prepared and tested. Considering limitation of the testing facility, the column has a square cross-section of 300×300 mm^2 and an overall height of 2,130 mm. The beam with a rectangular cross-section of 250×300 mm^2 has a total length of 2,800 mm. Reinforcement in beam and column was designed based on the Chinese code GB50010 [5] and satisfy requirements in terms of minimum reinforcement ratio, strong column-weak beam criteria and shear demand. The beam is reinforced symmetrically at the top and bottom with 3Φ14 bars (i.e. reinforcement ratio ρ_s=ρ_s'=0.6%). The ratio of the column section height

over the diameter of beam longitudinal reinforcement is controlled over 20 to ensure satisfactory bonding condition within joint cores. The column has 8Φ16 bars (i.e. reinforcement ratio 1.8%) as longitudinal reinforcement. Two-legged Φ10 stirrups spaced at every 100 mm were placed as transverse reinforcement for both beam and column. The first stirrups at the beam and column were placed at 50 mm and 25 mm from the joint edges, respectively. The concrete cover was controlled as 25 mm for all the specimens.

The joint reinforcement detail is also shown in Figure 2. The control specimen JC was reinforced with conventional three layers of two-legged Φ10 stirrups in accordance with the design code [5]. The other four specimens J-0.25h_b, J-0.5h_b, J-0.75h_b and J-1.0h_b adopted the novel joint reinforcement detail. Two pairs of Φ12 steel bars (*i.e.* 4 bars in total) were assigned, with different lengths of the anchorage segments L_a for each specimen. The L_a was controlled at $0.25h_b$ ($\approx$ 90 mm), $0.5h_b$ ($\approx$ 175mm), $0.75h_b$ ($\approx$ 265 mm) and $1.0h_b$ ($\approx$ 350 mm), as indicated by their names. Here, h_b is the height of the beam cross-section. In addition, one layer of two-legged Φ10 stirrup (volumetric stirrup ratio 0.65%) was remained at the middle height of the joint core for necessary concrete confinement [14,29]. The plastic hinges were expected to form at the ends of the anchorage segments. Consequently, the length of the anchorage segments is considered to be equal to the relocating distance when plastic hinge relocation is achieved. In addition, the flexural strength ratio of columns to beams in the BCJ specimens with the novel reinforcement detail also meets the requirement in the design code so as to avoid premature column failure. It should be noted that test results of specimens JC and J-0.5h_b were reported in the previous paper (i.e. specimens J1 and J3 in [14]) and are included in this paper for comparison.

The length of anchorage segments L_a also affects their effectiveness in contributing to flexural capacity and subsequently the relocation of plastic hinges. According to GB50010 [5], the

anchorage length L_a of deformed bars with mechanical anchors under tension can be determined by Eq. (1) .

$$L_a = \zeta_E \times 0.084d \times f_y/f_t \quad (1)$$

where $\zeta_E = 1.15$ is the amplification factor under seismic load. d is the bar diameter. f_y and f_t are the yielding strength of steel bar and the tensile strength of concrete, respectively. Hence, the calculated required anchorage length L_a of the novel reinforcement detail is 208 mm in this study, which falls between the anchorage lengths for specimens J-0.5h_b (175 mm) and J-0.75h_b (265 mm).

Hot-rolled deformed steel bars in one batch were selected for fabricating the steel cages. Their yield and ultimate strengths in different diameters were measured by uniaxial tensile test. The BCJ specimens were casted with ready-mixed concrete in one batch. For each specimen, 100 mm cubes were prepared to evaluate their compressive strength on the loading date. Material strengths of steel reinforcement and concrete are given in Table 1. The averaged compressive strength of concrete in the five specimens is 44.8 MPa with a standard deviation of 2.1 MPa, indicating that the influence of concrete strength on the performance of beam-column joint specimens is negligible.

Table 1: Material strengths of reinforcement and concrete.

Reinforcement			Concrete	
Diameter (mm)	Yielding strength (MPa)	Ultimate strength (MPa)	Specimen	Compressive strength (MPa)
Φ10	450	635	JC	43.6
Φ12	453	645	J-0.25h_b	47.1
Φ14	443	668	J-0.5h_b	45.6
Φ16	460	650	J-0.75h_b	42.0
			J-1.0h_b	45.9

3.2 Test setup, instrumentation and loading scheme

Figure 3 shows the test setup for the BCJ specimens. The bottom of the column was hinged to the testing frame installed on the strong floor, while both ends of the beam were restrained in vertical displacement only. A hydraulic jack was adopted to apply axial load on the column through post-tensioning four high strength steel rods. A servo-hydraulic actuator connecting to the column top through a hinge was adopted to apply horizontal load. The distances between inflection points were 2,400 mm for beams and 2,130 mm for columns.

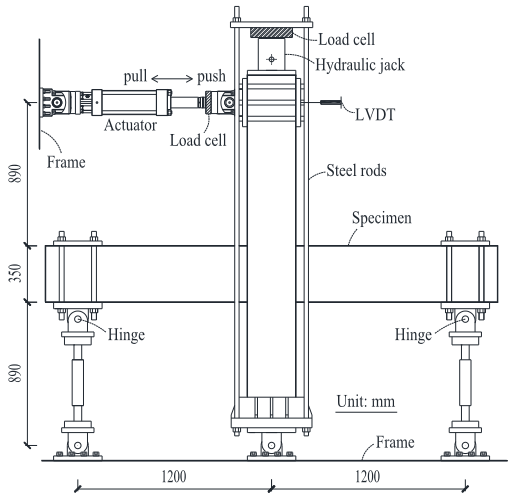

Figure 3: Test setup for BCJ specimens.

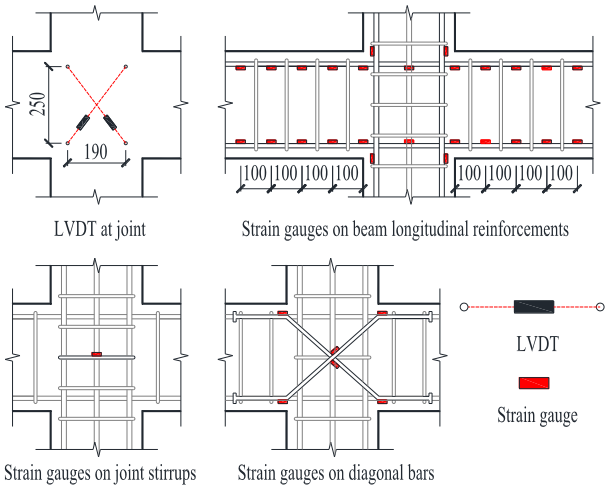

Figure 4: Instruments on BCJ specimens.

A wire linear variable displacement transducer (LVDT) was installed on the upper column tip to monitor the applied horizontal displacement. A load cell was positioned between the actuator and specimen to record the horizontal reaction force. Besides, a pair of LVDTs was installed in the joint core for determining the joint shear deformation as shown in Figure 4. Strain gauges were also attached to the beam longitudinal reinforcement, the diagonal bars, and the stirrups to monitor their strains. Arrangement of strain gauges on reinforcement is also shown in Figure 4.

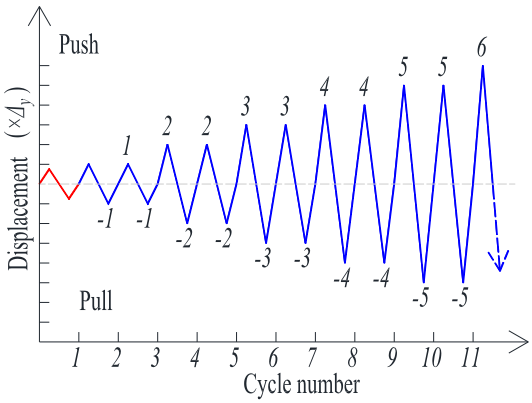

Figure 5: Loading sequence.

Horizontal cyclic load was applied to the BCJ specimens after imposing the axial load on the columns. The axial load was controlled at $0.2f_c'A_g$ and maintained constant throughout the test. Here f_c' is the cylindrical compressive strength of concrete and is taken as 0.8 times the measured cubic compressive strength [30]. A_g is the gross area of column section. Afterwards, the horizontal displacement was applied according to the loading sequence in Figure 5. During the first cycle, the horizontal displacement was gradually applied until the beam reached 75% of its nominal bending moment capacity, and the corresponding horizontal displacement was recorded as $\Delta_{0.75}$. The nominal yielding displacement was subsequently calculated as $\Delta_y=\Delta_{0.75}/0.75$ based on linear extrapolation. The first cycle finished after reversing the horizontal displacement to $-\Delta_{0.75}$ and then returning to the neutral position. Starting from the second loading cycle, the horizontal displacement levels were determined by increments of Δ_y,

with each horizontal displacement level repeated twice. The tests continued until the horizontal load decreased to 80% of recorded peak load.

4. Experimental results and discussion

4.1 General behaviour and failure modes

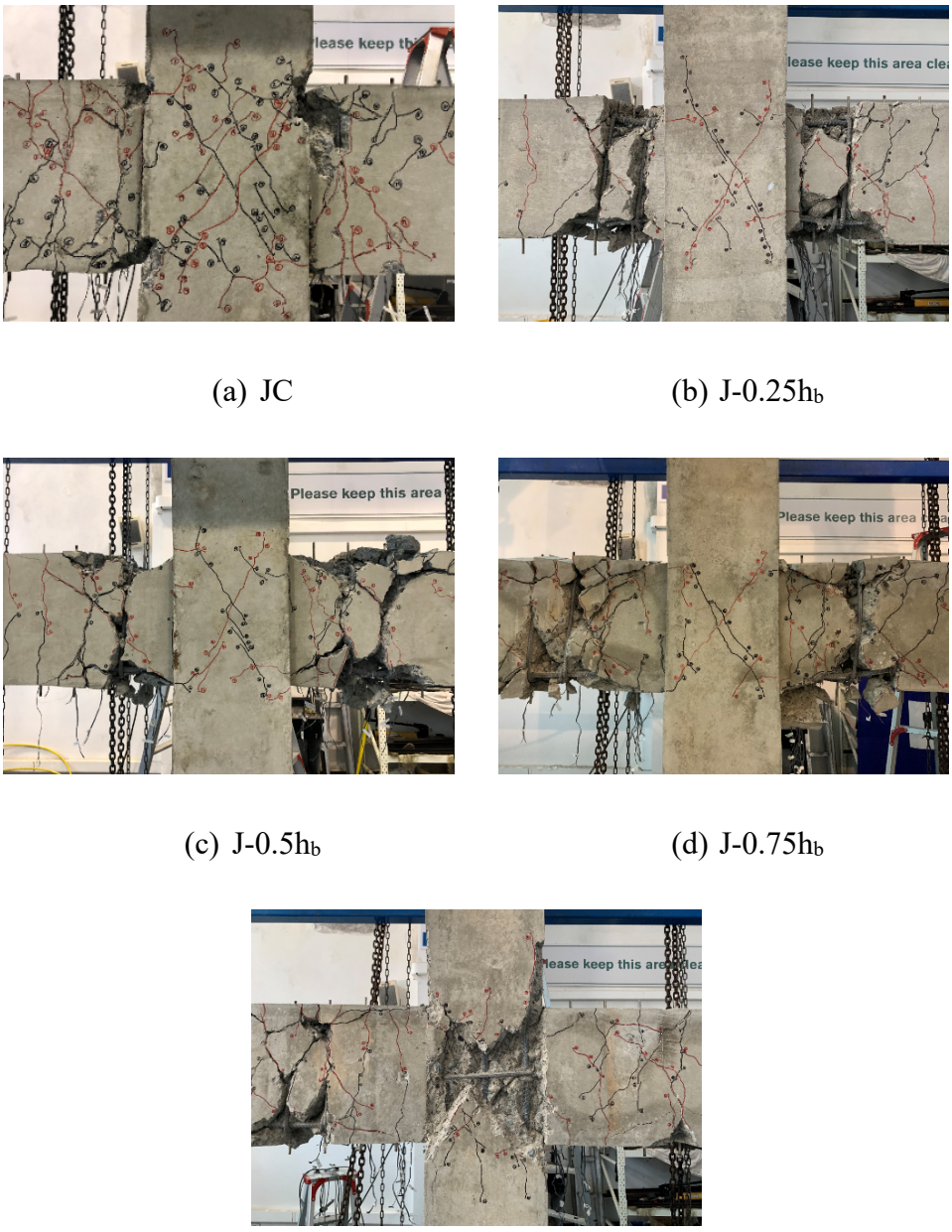

(a) JC (b) J-0.25h_b

(c) J-0.5h_b (d) J-0.75h_b

(e) J-1.0h_b

Figure 6: Cracks and failure modes of BCJ specimens.

(Note: Specimens JC and J-0.5h_b are named J1 and J3 in [14], respectively)

Figure 6 shows the crack patterns and failure modes of the BCJ specimens. Specimen JC failed with plastic hinges formed at the beam-joint interfaces and cracks appeared inside the joint core. In general, specimens J-0.25h_b, J-0.5h_b and J-0.75h_b exhibited similar cracking process during the test. At the initial loading stage, flexural cracks were first found on the beams. With the increased horizontal displacement, more flexural cracks formed on the beams and propagated through the depth of beam sections. The main flexural cracks were found at the anchorage ends of diagonal bars, due to the fact that the addition of the anchorage segments enhanced the flexural capacities of sections at the beam ends. The first diagonal crack inside joint core was observed at 30 mm displacement for specimens J-0.25h_b and J-0.5h_b, while it occurred earlier at 15 mm displacement for specimen J-0.75h_b. This is probably due to the slightly lower strength of concrete in specimen J-0.75h_b. As the increase of horizontal displacement, the cracks inside the joint cores continuously developed in terms of both quantity and length. Although specimen J-0.75h_b showed fewer joint cracks than specimens J-0.25h_b and J-0.5h_b, those joint cracks in the three specimens hardly grew in width. This indicates that shear failure could still be avoided in BCJs with different anchorage lengths for the novel reinforcement detail, despite of the relatively fewer stirrups inside joint cores. Afterwards, the plastic hinges formed at the anchorage ends of diagonal bars. At the later loading stage, there were severe concrete crushing and spalling at the plastic hinge zones, followed with the buckling of the beam longitudinal reinforcement. Specimens J-0.25h_b, J-0.5h_b and J-0.75h_b failed in beam flexure with relocated plastic hinges. In summary, the plastic hinges can be relocated by different distances between 0.25h_b and 0.75h_b due to the various anchorage lengths, leading to fewer joint cracks as compared to specimen JC. However, variation of the relocating distance has a negligible effect on the crack development and failure modes of specimens J-0.25h_b, J-0.5h_b and J-0.75h_b.

The cracking behaviour of specimen J-1.0h_b at the initial loading stage was similar to that of other specimens. Multiple flexural cracks occurred on the beams with the widest ones found at the anchorage ends of diagonal bars. The first joint crack was also observed at the displacement of 30 mm. However, specimen J-1.0h_b failed in a different mode as compared with other specimens. On the left beam, significant concrete crushing and spalling was found at the beam section corresponding to the anchorage ends, indicating that plastic hinge relocation was achieved. However, the damage on the right beam mainly concentrated at the beam-joint interface, and the plastic hinge was not relocated. Moreover, specimen J-1.0h_b suffered a severe damage inside the joint core with more diagonal cracks. As the joint cracks experienced repeated opening and closing, massive concrete spalling inside the joint core was observed at the advanced loading stage. Overall, specimen J-1.0h_b failed in a hybrid mode with relocated plastic hinge forming on the left beam followed by joint shear failure. This means that further increasing the length of the anchorage segments may result in unsuccessful plastic hinge relocation. More importantly, improper design for the relocating distance can turn the failure mode from beam plastic hinge to joint shear.

4.2 Hysteretic behaviour

Figure 7 shows the hysteretic loops of horizontal load to displacement at the upper column tip for BCJ specimens. At the early loading stage, the horizontal load ascends linearly with the horizontal displacement. Consequently, the areas of hysteretic loops are relatively small before the yielding of the BCJ specimens. As the specimens entered yielding stage, inelastic deformations by concrete cracking and reinforcement yielding occur in all the BCJ specimens. The loading and reloading stiffness (i.e. the slope of hysteretic loops) gradually decreases, and the areas enclosed in the hysteretic loops enlarge with the horizontal displacement.

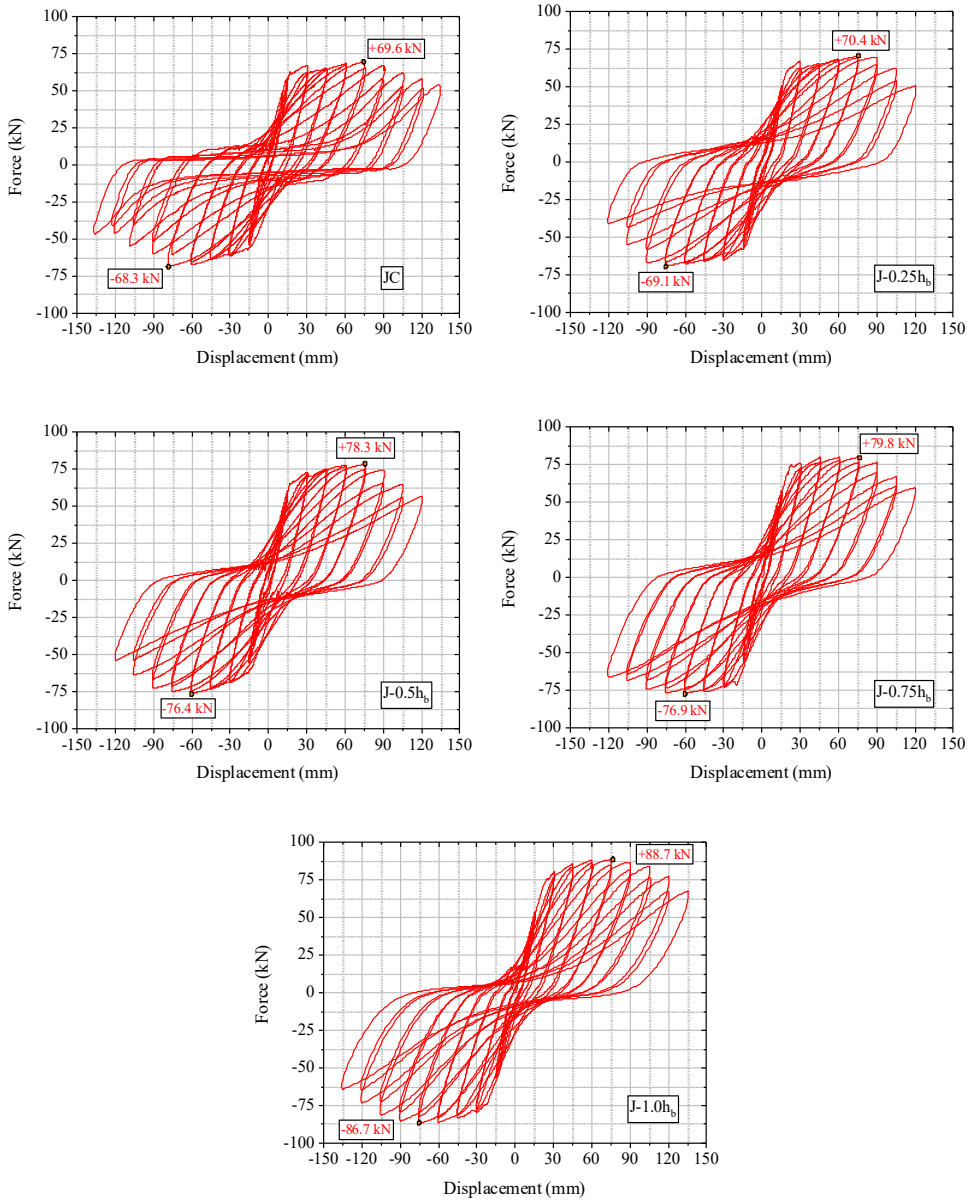

Figure 7: Hysteretic loops of BCJ specimens.

(Note: Specimens JC and J-0.5h_b are named J1 and J3 in [14], respectively)

The specimens J-0.25h_b, J-0.5h_b and J-0.75h_b have similar shape of hysteretic loops as they have comparable cracking behaviour and failure mode. Differently, the hysteretic loops of specimens JC and J-1.0h_b are narrower with smaller areas enclosed in those loops than those of the other specimens, indicating a more severe pinching phenomenon in both specimens. This is attributed to the deteriorated bonding condition of beam longitudinal reinforcement inside the joint core, due to the plastic hinges formed at the beam-joint interfaces and the more severe

damage of joint core. In general, it can be found that plastic hinge relocation can weaken the pinching effect, and increasing the relocating distance for plastic hinges from $0.25h_b$ up to $0.75h_b$ marginally affects the hysteretic behaviour of BCJ specimens. However, relocating plastic hinges by $1.0h_b$ may trigger the joint shear failure and results in an obvious pinching phenomenon similar to that in specimen JC. Thus, the relocating distance for plastic hinge should be designed below the limit inducing joint shear failure.

4.3 Envelope curves and ductility

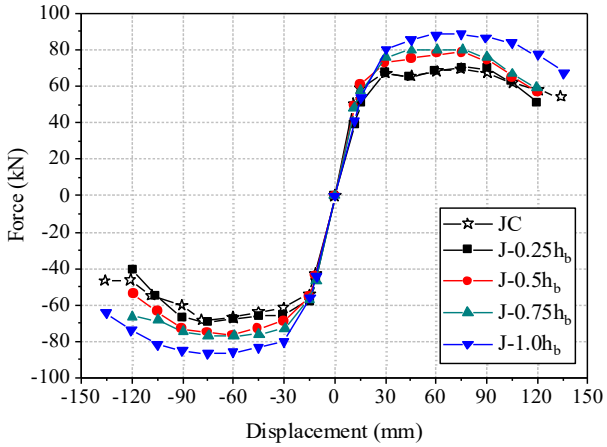

Figure 8: Envelope curves of the hysteretic loops.

Figure 8 shows the envelope curves of hysteretic loops for BCJ specimens. At the initial loading stage (e.g. at displacement less than 15 mm), the loads for the specimens are comparable and the slopes of the curves are nearly identical. These curves are almost overlapped, indicating that the relocating distance of plastic hinges has negligible effects on the envelope curves at this stage. When the horizontal displacement reaches 30 mm, the differences in the five envelope curves become evident as the yielding of specimens begins. Under the same displacement, the BCJ specimens with the proposed reinforcement detail show higher loads due to the decrease of force arm from the beam inflection point to the plastic hinge sections. In addition, increasing the relocating distance further enhances the loading capacity of BCJ specimens. For example, the loading capacities of specimens J-0.25h_b and J-1.0h_b are 2% and

27% higher than that of specimen JC, respectively. However, this enhancement in the loading capacity is probably limited by the joint shear strength, as indicated by the joint shear failure in specimen J-1.0h_b. After reaching the loading capacities, the loads of all the specimens start to drop until their complete failure at displacements of 120 mm or 135 mm, which indicates all specimens have a comparable deformation capacity.

Table 2 shows the displacement ductility factors μ for BCJ specimens. Here, the ductility factor is defined as the ratio of ultimate displacement Δ_u over the yielding displacement Δ_y. The ultimate displacement is taken as the displacement corresponding to 20% drop of the loading capacity. The yielding displacement is calculated according to energy balance method [31]. Specimen JC with conventional stirrups achieved a ductility factor of 4.9, while specimens J-0.25h_b, J-0.5h_b and J-1.0h_b exhibit reduced ductility factors around 4.2. However, the ductility factor of specimen J-0.75h_b increases to 4.8, which is comparable to that of specimen JC. This indicates that relocating plastic hinges by a distance within 0.5h_b has a marginal impact on the ductility of BCJ specimens. However, increasing the relocating distance to 0.75h_b can recover the ductility to the level for the code-designed specimen JC. This can be attributed to the less damage within the joint core so that the behaviour of specimen J-0.75h_b is more dependent on the ductile flexural failure of beam. Further increasing the anchorage length to 1.0h_b decreases the ductility. This is attributed to the joint shear failure and increased yielding displacement. As seen in Table 2, specimen J-1.0h_b exhibits a much higher yielding displacement than the other BCJ specimens. Overall, all the specimens with plastic hinge relocation show slightly reduced ductility than the control specimen, and the relocating distance needs to be properly controlled within a certain range for achieving higher ductility of BCJs.

Table 2: Calculated displacement ductility of BCJ specimens.

Specimen	Δ_y (mm)		Δ_u (mm)		μ
	Push	Pull	Push	Pull	*(mm/mm)*
JC	21.7	26.8	129.1	108.4	4.9
J-0.25h_b	28.1	22.5	112.8	105.1	4.3
J-0.5h_b	24.7	27.1	109.3	108.6	4.2
J-0.75h_b	24.6	23.6	111.1	121.4	4.8
J-1.0h_b	31.5	28.7	130.4	127.1	4.3

4.4 Energy dissipation

Figure 9 shows the relationship between cumulative energy dissipation and the horizontal displacement of BCJ specimens. In general, the cumulative energy dissipation of all the BCJ specimens gradually increase as the horizontal displacement increases. The cumulative energy dissipation of BCJ specimens are almost the same before 30 mm displacement, since the behaviour of specimens at this stage is dominated by the flexural cracking on the beams. This process absorbs limited energy as compared to reinforcement yielding and concrete crushing. Afterwards, the cumulative energy dissipation increases in an ascending rate as the BCJ specimens enter the yielding stage.

Overall, the energy dissipation of the specimens with the plastic hinge relocation is higher than that of specimen JC. More specifically, the energy dissipation of specimens J-0.5h_b and J-0.75h_b is higher than that of specimen J-0.25h_b. This means increasing the relocating distance from 0.25h_b to 0.5h_b and 0.75h_b is beneficial for the BCJ specimen to dissipate energy. This can be attributed to the following two factors. Firstly, specimens J-0.5h_b and J-0.75h_b sustain higher loads than specimen J-0.25h_b at the same horizontal displacement. Secondly, the longer relocating distance increases the development length between two plastic hinges on beams, which weakens the yielding strain penetration into joint core and improves bonding condition

of beam longitudinal reinforcement. Meanwhile, specimens J-0.5h_b and J-0.75h_b possess similar energy dissipation capacity, indicating that increasing the relocating distance of plastic hinges from 0.5h_b to 0.75h_b has a negligible impact on the energy dissipation of BCJs. Although the longer relocating distance can further reduce yielding penetration into joint core and improve the bonding condition of beam longitudinal reinforcement [17,20], in this case their bonding condition does not dominate the energy dissipation of these two specimens. The beam longitudinal reinforcement in all the specimens has met the anchorage requirement (i.e. ratio of the column section depth to the bar diameter) specified in the design code. Consequently, energy dissipation of the specimens highly depends on beam plastic hinges with the same reinforcement. On the other hand, specimen J-1.0h_b shows lower energy dissipation capacity than specimens J-0.25h_b, J-0.5h_b and J-0.75h_b due to the failure of plastic hinge relocation on the right beam and joint shear failure. The unachieved plastic hinge relocation also leads to higher yielding penetration into the joint core and deteriorates the bonding condition of longitudinal reinforcement. This indicates that the relocating distance should be controlled lower than a limit to ensure the plastic hinge relocation and avoid joint shear failure. However, as specimen J-1.0h_b possesses the highest deformation among the four specimens adopting the proposed reinforcement detail, its total energy dissipation capacity at failure is comparable to that of specimens J-0.25h_b, J-0.5h_b and J-0.75h_b. Therefore, the plastic hinge relocation can increase the cumulative energy dissipation of BCJs regardless of the diferent relocating distances.

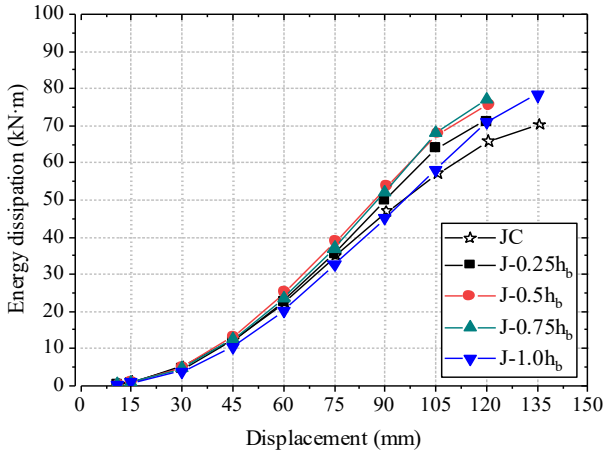

Figure 9: Cumulative energy dissipation of BCJ specimens.

4.5 Stiffness degradation

Figure 10 shows the stiffness against the horizontal displacement of BCJ specimens. As illustrated in Figure 10, the stiffness is calculated as the slope of the line connecting positive and negative peak load points in the first cycle at different horizontal displacements. For all the specimens, the stiffness degrades in a similar manner as the horizontal displacement increases. The initial stiffness of specimens is comparable, indicating that the different anchorage length negligibly affects their initial stiffness. As the horizontal displacement increases, BCJ specimens with plastic hinge relocation exhibit higher stiffness than specimen JC. Meanwhile, a longer relocating distance for plastic hinges results in slower stiffness degrading rate. For instance, among the four BCJ specimens with the plastic hinge relocation, specimens J-0.25h_b and J-1.0h_b exhibit the lowest and highest stiffness at the same horizontal displacement, respectively. This is attributed to the increased stiffness of beams with the longer anchorage segments. Moreover, the longer relocating distance increases the development length of beam longitudinal reinforcement and reduces its yielding penetration into the joint core. This consequently improves the bonding condition of longitudinal reinforcement and delays the stiffness degradation of BCJ specimens. At the late loading stage, the behaviour of specimens was dominated by the beam plastic hinges. Hence, the stiffness of specimens at the failure

condition tends to be similar. Generally, the plastic hinge relocation can increase the stiffness of BCJs, especially for those with a longer relocating distance is adopted.

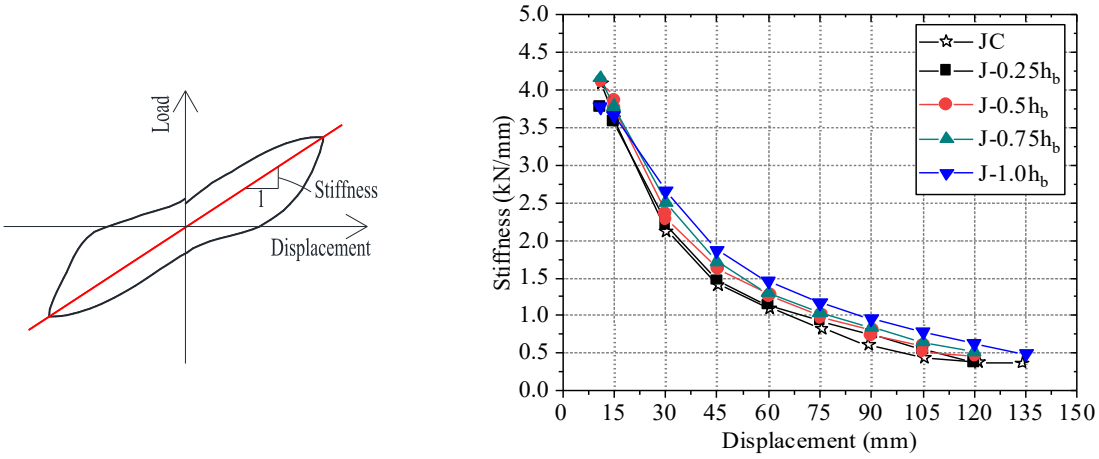

Figure 10: Stiffness degradation of BCJ specimens.

4.6 Joint shear deformation

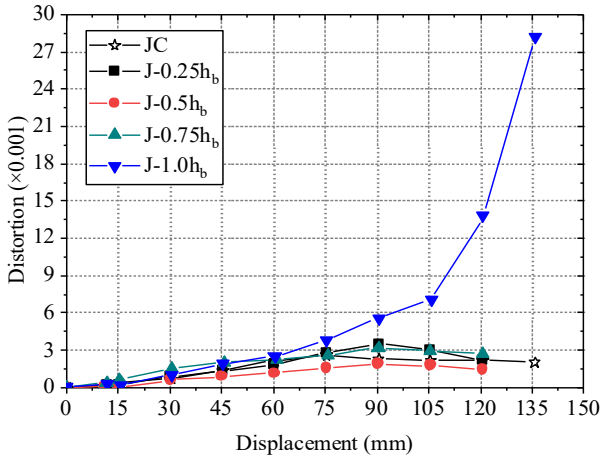

Figure 11: Joint shear deformation of BCJ specimens.

Figure 11 shows the joint shear deformation against the horizontal displacement of BCJ specimens. The joint shear deformation is calculated based on the readings of two diagonal LVDTs in the joint cores. The joint shear deformations of specimens JC, J-0.25h_b, J-0.5h_b and J-0.75h_b increase as the horizontal displacement increases, followed by slight reduction at the later loading stage. Specimens J-0.25h_b, J-0.5h_b and J-0.75h_b show comparable shear

deformation to specimen JC. Specially, specimen J-0.5h_b exhibits the lowest joint shear deformation, which is around 50% lower than that in specimen J-0.25h_b at the same displacement level. This indicates that relocating plastic hinges with a longer distance can reduce the strain penetration of beam longitudinal reinforcement into the joint cores and subsequently decreases the deformation of joint cores. When the relocating distance is further increased to 0.75h_b, however, the joint shear deformation of specimen J-0.75h_b increases and is comparable to that of specimen J-0.25h_b. With farther relocated plastic hinges, the yielding strain penetration in specimen J-0.75h_b is further reduced as indicated by the strain of beam longitudinal reinforcement in section 4.8. However, the longer relocating distance also amplifies the bending moments at the beam-joint interfaces that tend to increase the joint shear deformation. It can be inferred that the negative effect due to amplified bending moment is more significant than the positive influence contributed by reduced yielding strain penetration. Specimen J-1.0h_b exhibits the highest joint shear deformation among the five BCJ specimens, which is obviously related to the observed damage inside the joint core. Moreover, the failure of plastic hinge relocation on the right beam could also increase the deformation of joint core. As the occurrence of joint shear failure at the later loading stage, the joint shear deformation of specimen J-1.0h_b dramatically increases and is much higher than that of the other four BCJ specimens. Overall, increasing the relocating distance for plastic hinges first mitigates but then increases joint shear deformation.

4.7 Strain of joint stirrups

Figure 12 shows the relationship between the strains of joint stirrup and the horizontal displacement for BCJ specimens. Specimens JC and J-0.75h_b exhibits a higher strain than the other specimens as the horizontal displacement reaches 15 mm, which is caused by ealier joint cracking due to the slightly lower concrete strength. Nevertheless, as joint cracks occurred in all specimens at displacement 30 mm, the strains of joint stirrups after cracking in all BCJ

specimens tend to be consistent. Afterwards, the strains of stirrups in specimens JC, J-0.25h_b, J-0.5h_b and J-0.75h_b increase as the horizontal displacement increases, followed with slight decreases. This indicates that the stirrups are sufficient for shear resistance inside the joint core. Specifically, the strain in specimen JC is higher than that in specimen J-0.25h_b, followed by specimens J-0.75h_b and J-0.5h_b. Since the stirrups contribute to the joint shear resistance, this also implies the input shear forces to the joint cores follow in the same trend. The decrease in strains of stirrups at the later loading stage in specimens JC, J-0.25h_b, J-0.5h_b and J-0.75h_b is mainly caused by the reduced truss mechanism as the bonding condition of beam longitudinal reinforcement inside joint cores deteriorates under cyclic load. On the other hand, the strain of stirrup in specimen J-1.0h_b dramatically increases and exceeds the yielding value after the 75 mm horizontal displacement. This agrees well with the observed joint shear failure and reflects that the stirrups inside the joint core are insufficient. In general, the plastic hinge relocation reduces the strain of stirrups inside the BCJ cores, while increasing the relocating distance first reduces and then increases the strain of stirrups. This again highlights that the relocating distance for plastic hinges shall fall within proper limits to reduce the induced joint shear force.

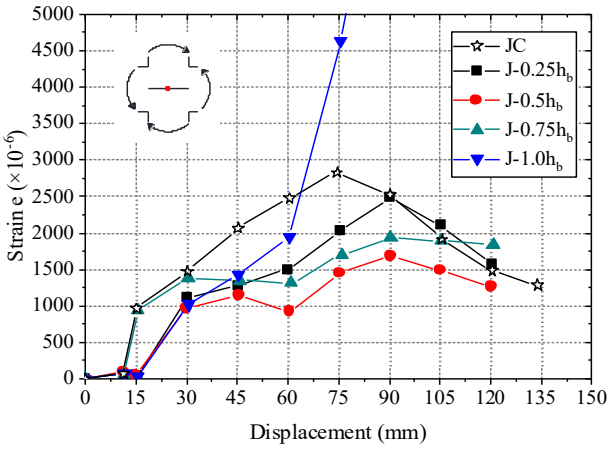

Figure 12: Joint stirrup strain of BCJ specimens.

4.8 Strain distributions of beam longitudinal reinforcement

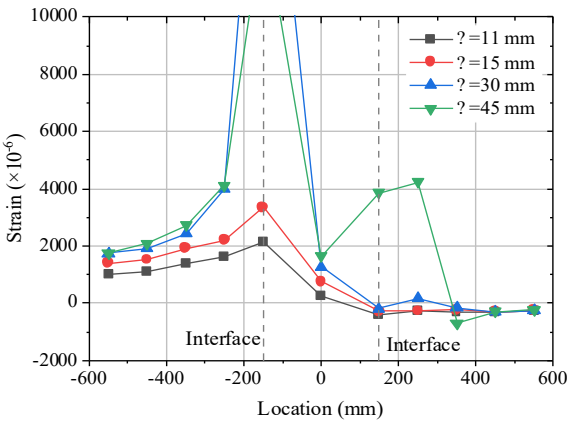

(a) JC

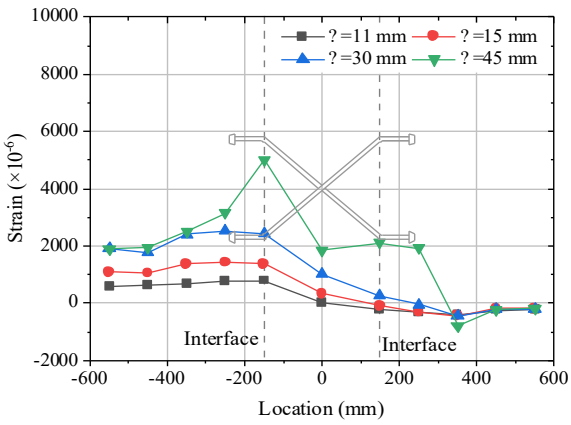

(b) J-0.25h_b

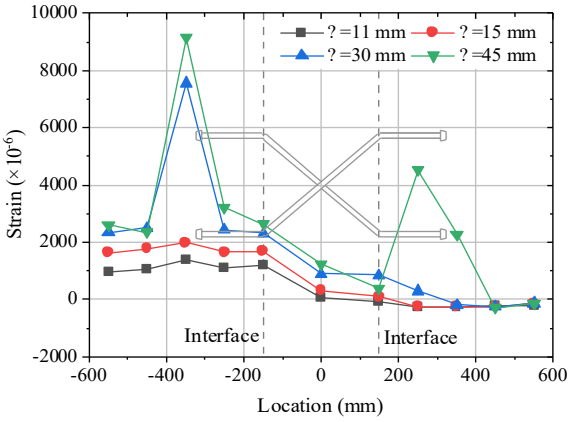

(c) J-0.5h_b

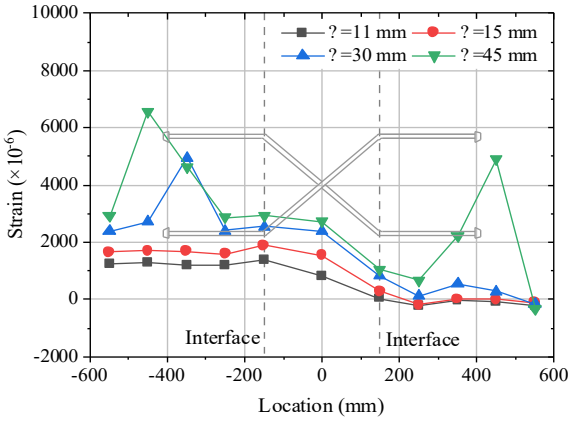

(d) J-0.75h_b

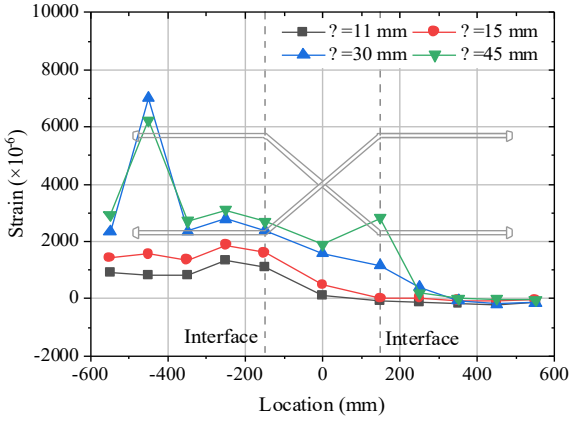

(e) J-1.0h_b

Figure 13: Strain distributions of beam longitudinal reinforcement.

(Note: Specimens JC and J-0.5h_b are named J1 and J3 in [14], respectively)

Figure 13 shows the strain distributions of top beam longitudinal reinforcement under the push loading. Here, the x and y-axes represent the location of strain gauges to the column centreline and corresponding strain values, respectively. Only the results at the horizontal displacement up to 45 mm are shown due to the failure of some strain gauges after reversed reinforcement yielding. At the initial loading stage, the strains of beam longitudinal reinforcement in all the BCJ specimens remain elastic. At 15 mm displacement, the beam longitudinal reinforcement in specimen JC yield at the left beam-joint interface. As the horizontal displacement reaches 30 mm, yielding of beam longitudinal reinforcement occurs in all the specimens but at different locations, due to the plastic hinge relocation and different lengths of the anchorage segments in each specimen. For instance, the peak strain of longitudinal reinforcement in specimens JC and J-0.25h_b is observed at the location of -150 mm (i.e. left beam-joint interface). While for the other specimens, the location with the highest strain of bars is shifted to the designed beam sections for plastic hinges. For example, the peak strain of longitudinal reinforcement in specimen J-0.5h_b is located at -350 mm (i.e. 200 mm from the beam-joint interface). When the horizontal displacement is further increased to 45 mm, the strains of longitudinal reinforcement at the left side continually grow, while those on the right side also exhibit peaks. This is because the tensile reinforcement strains cannot be recovered once the plastic hinges have formed. The peak reinforcement strains at left and right sides for specimens JC, J-0.25h_b, J-0.5h_b and J-1.0h_b are symmetrically located as the relocation was achieved on both left and right beams. Nevertheless, the highest strain in specimen J-1.0h_b is found at -450 mm and 150 mm. This confirms that the plastic hinge relocation is achieved only on the left beam in specimen J-1.0h_b.

Compared to the other specimens, specimen J-0.25h_b shows higher strains of longitudinal reinforcement at the beam-joint interface. This indicates that the longer anchorage length of the proposed reinforcement detail can reduce the yielding strain penetration of beam longitudinal reinforcement into the joint core. On the other hand, further increasing the

anchorage length from $0.5h_b$ to $0.75h_b$ or $1.0h_b$ increases the strains of longitudinal reinforcement within the joint cores. It reflects that the longer anchorage length increases the induced bending moment at the beam end and has a negative impact on the performance of joint core.

4.9 Strain of the novel reinforcement detail

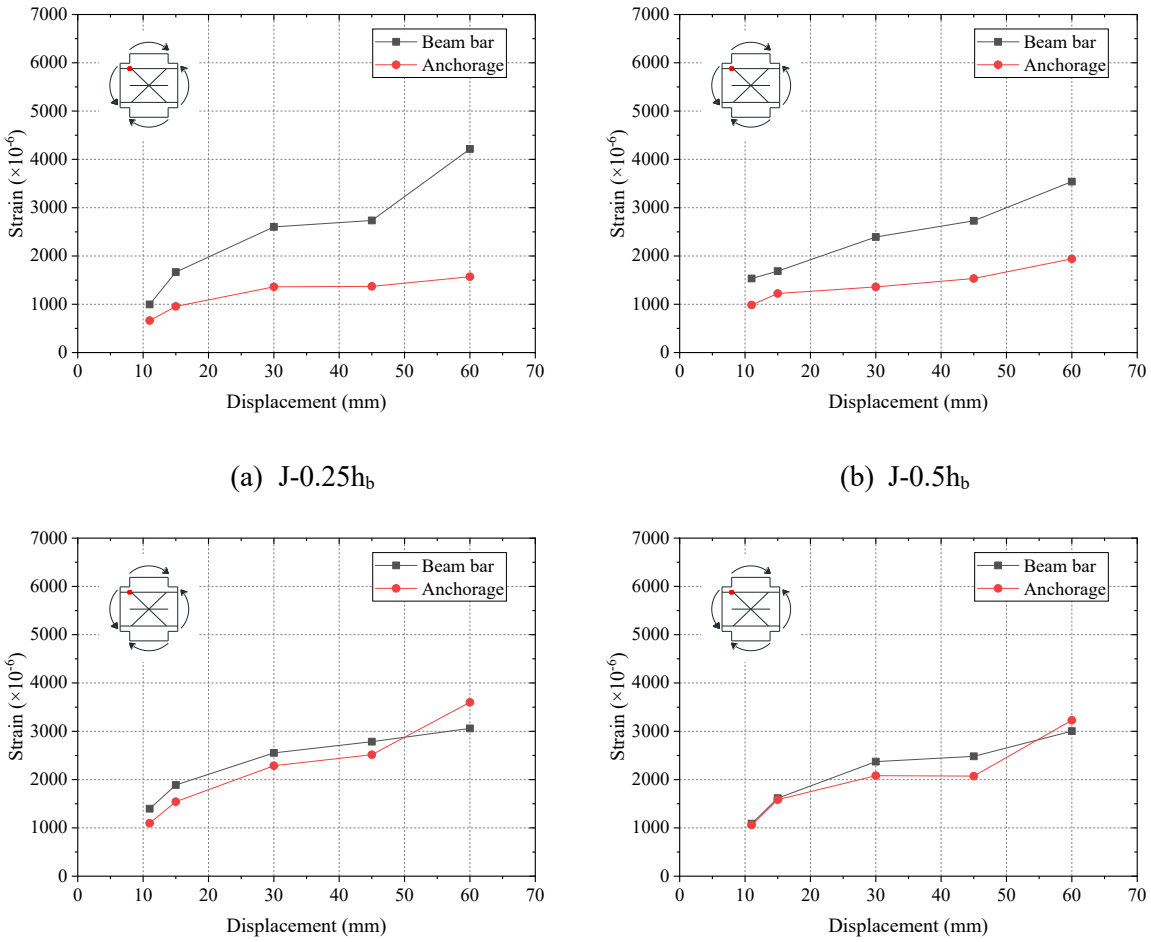

(a) J-0.25h$_b$ (b) J-0.5h$_b$

(c) J-0.75h$_b$ (d) J-1.0h$_b$

Figure 14: Strain of anchorage segments at the beam-joint interfaces.

Figure 14 shows the strains of the anchorage segments at the beam-joint interfaces in BCJ specimens under various horizontal displacements. The strains of beam longitudinal reinforcement at the same position are also plotted for comparison. Generally, both beam longitudinal reinforcement and the anchorage segments contribute to flexural resistance of the

beam sections, and their strains increase with the horizontal displacement. In specimens J-0.25h_b and J-0.5h_b, the strains on the anchorage segments are nearly half of those on the beam longitudinal reinforcement. This means the anchorage segments in these two specimens are less effective than beam longitudinal reinforcement in contributing to the flexural resistance of sections at the beam-joint interfaces. Differently, the strains on the beam longitudinal reinforcement and the anchorage segments tend to be consistent in specimens J-0.75h_b and J-1.0h_b. This higher strain compatibility in specimens J-0.75h_b and J-1.0h_b indicates that the contribution of the anchorage segments to the flexural resistance of the beam sections is enhanced, which is mainly attributed to the improved stress development in the longer anchorage segments. As the required anchorage length L_a estimated by Eq. (1) is between 0.5h_b and 0.75h_b, Eq. (1) is recommended to calculate the minimum required length of anchorage segments in order to maximize their effectiveness. Overall, increasing the anchorage length is beneficial in improving the efficiency of the anchorage segments in contributing to the flexural resistance of beams. Moreover, the forces acting on the anchorage segments are transmitted to the diagonal segments and self-balanced, which can diverge higher forces from the joint core by the proposed reinforcement detail.

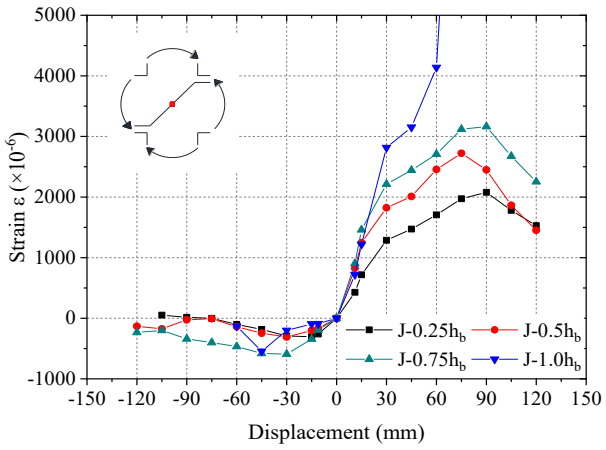

Figure 15: Strain of diagonal segments of the novel reinforcement detail.

Figure 15 shows the strains of the diagonal segments of the novel reinforcement detail under various horizontal displacements. The diagonal segments are subjected to much higher tensile strain than compressive strain, indicating that the diagonal segments are more effective in balancing the tensile force rather than compressive force. Under the same horizontal displacement, the tensile strains of diagonal segments increase with the relocating distance for plastic hinges. The diagonal bars in specimen J-0.25h_b are within elastic strain range, while those in the other three BCJ specimens reach the yielding level. The increase of strains is attributed by the enhanced force transmitted from the anchorage segments. It also indicates that the longer anchorage length is helpful in further utilizing the strength of the diagonal segments. The strain of diagonal bars in specimen J-1.0h_b reaches the yielding value and increases dramatically after the displacement of 60 mm, which agrees with the joint shear failure observed in specimen J-1.0h_b.

5. Analytical model

5.1 Plastic hinge relocation mechanism

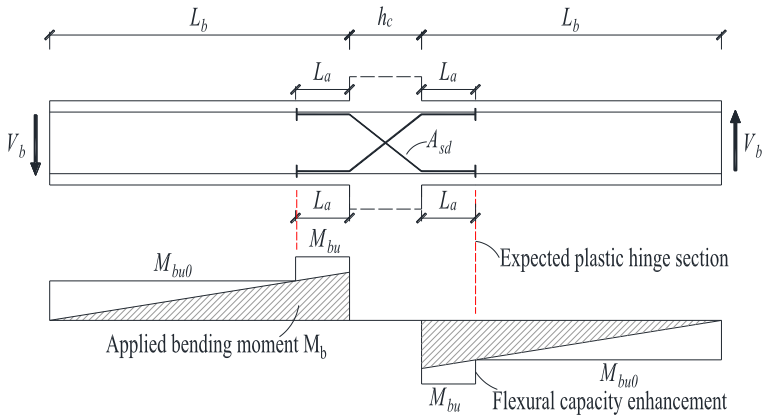

Figure 16: Illustration of plastic hinge relocation.

Figure 16 shows the analytical model for the plastic hinge relocation mechanism in BCJs. The applied bending moment along beam in a BCJ is marked in shadow. If the plastic hinges are assumed to be formed at the ends of the anchorage segments, the applied bending moment M_{bh}

at the ends of the anchorage segments should be equal to the flexural capacity M_{bu0} without the enhancement by the anchorage segments as shown in Eq. (2).

$$M_{bh}=M_{bu0} \tag{2}$$

The beam shear force V_b and the bending moment M_{bj} at the beam-joint interfaces can be subsequently determined by Eqs. (3) and (4), respectively.

$$V_b=M_{bu0}/(L_b-L_a) \tag{3}$$

$$M_{bj}=V_b\times L_b= M_{bu0}\times L_b / (L_b-L_a) \tag{4}$$

where L_b is the distance from beam inflection point to the beam-joint interface, and L_a is the length of the anchorage segments.

To ensure the plastic hinge relocation, the enhanced flexural capacity of beam sections M_{bu} should exceed the applied bending moment M_{bj} at the beam-joint interfaces as given in Eq. (5).

$$M_{bu} > M_{bj} \tag{5}$$

The flexural capacity M_{bu} and applied bending moment M_{bj} at the beam-joint interfaces are correlated to the anchorage length L_a. With a small anchorage length, the efficiency of the anchorage segments in enhancing the flexural resistance at beam ends is relatively poor. A minimum length of anchorage segments has to be specified based on Eq. (1). On the other hand, increasing the anchorage length reduces the force arm measured from the beam inflection point to the expected plastic hinge section and consequently increases the beam shear force, which further amplifies the applied bending moment M_{bj} at the beam-joint interfaces. To satisfy Eq. (5), the flexural capacity at beam ends has to be further enhanced by adopting the proposed reinforcement detail in a higher quantity or larger diameter. To relocate the plastic hinges in BCJs, the anchorage length L_a has to be determined with the consideration of its impacts on the applied bending moment M_{bj} and the flexural capacity M_{bu} at the beam-joint interfaces.

5.2 Force self-balancing mechanism

The proposed reinforcement detail is able to balance the forces transferred through the diagonal segments which are unbonded to the joint concrete. The forces acting on the joint cores have to be determined for calculating the joint shear force. Figure 17 shows the sectional analysis for the beam-joint interface under bending. With the applied bending moment M_{bj}, the bottom longitudinal reinforcement and the anchorage segments are under tension, while those at top are under compression. For BCJs with relocated plastic hinges, M_{bj} can be calculated by Eq. (4). Otherwise, M_{bj} is taken as the flexural capacity at the beam-joint interface M_{bu}.

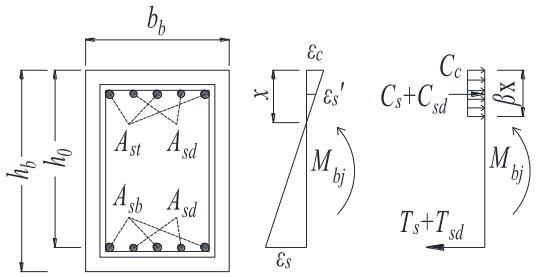

Figure 17: Sectional analysis for beam-joint interface under bending.

With plane section assumption for beam longitudinal reinforcement and concrete, the strain of concrete ε_c, top beam longitudinal reinforcement ε_s' and bottom beam longitudinal reinforcement ε_s can be correlated with a presumed section compressive zone depth x. The strains for the anchorage segments at bottom ε_{sd} and at top ε_{sd}' of the section can be estimated based on those for beam longitudinal reinforcement, with an effectiveness factor α, as shown in Eqs. (6) and (7). This factor α depends on the efficiency of the anchorage segments in contributing flexural resistance of the beam section. Based on the strain analysis, α can be taken as 0.5 for specimens J-0.25h_b and J-0.5h_b and 1.0 for specimens J-0.75h_b and J-1.0h_b.

$$\varepsilon_{sd} = \alpha\varepsilon_s \tag{6}$$

$$\varepsilon_{sd}' = \alpha\varepsilon_s' \tag{7}$$

Afterwards, the two equilibrium conditions in Eqs. (8)-(9) can be established to calculate the forces applied on concrete and the reinforcement, where T_s and T_{sd} are the tensile forces on bottom beam longitudinal reinforcement and the anchorage segments at bottom, respectively. C_s and C_{sd} are the compressive forces on beam longitudinal reinforcement and the anchorage segments at top, respectively. C_c is the compressive force on concrete. h_0 is section effective depth. a_s' is the distance from centroid of top longitudinal reinforcement to the top edge. βx is the equivalent section compressive depth. For the specimens in this study, the neutral axes are close to the compressive reinforcement due to the symmetrical beam reinforcement. As a result, the forces on compressive reinforcement are relatively small and can be neglected in a simplified section analysis.

$$T_s+T_{sd}= C_s+C_{sd}+C_c \tag{8}$$

$$(C_s+C_{sd})(h_0-a_s')+C_c(h_0-\beta x/2) = M_{bj} \tag{9}$$

With the forces on steel reinforcement and concrete determined, the joint shear force can be calculated excluding the forces balanced by the diagonal segments. Figure 18 shows the forces acting on a joint core. Here, C_{c1} to C_{c4} are the compressive forces of concrete. T_{s1} to T_{s4} are the tensile forces on beam and column longitudinal reinforcement. C_{s1} to C_{s4} are the compressive forces on beam and column longitudinal reinforcement. T_{sd1} and T_{sd2} are the tensile forces on the anchorage segments. C_{sd1} and C_{sd2} are the compressive forces on the anchorage segments.

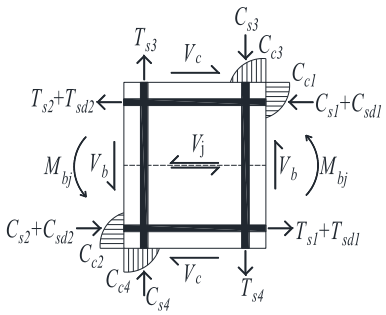

Figure 18: Forces acting on a joint core.

The forces on beam longitudinal reinforcement, namely T_{s1}, T_{s2}, C_{s1}, C_{s2}, are transmitted to the joint concrete by bonding and cause joint shear force. On the other hand, those forces on the anchorage segments (i.e. T_{sd1}, T_{sd2}, C_{sd1}, C_{sd2}) will be transferred to the diagonal segments and get self-balanced. In other words, those forces on the anchorage segments will not increase the joint shear force. Thus, the joint shear force V_j at the middle height of joint can be calculated by Eq. (10).

$$V_j = T_{s2} + C_{s1} + C_{c1} - V_c \tag{10}$$

where V_c is the column shear force.

5.3 Joint shear strength

The joint shear strength V_{ju} can be calculated based on Eqs. (11)-(14) in accordance with the code GB50010 [5]. It is provided by concrete, column axial force and joint stirrups. An upper limit of joint shear strength is also provisioned to prevent crushing of concrete strut.

$$V_{ju}=\min(V_{ju1}, V_{ju2}) \tag{11}$$

$$V_{ju1}=0.3f_c' b_j h_j/0.85 \tag{12}$$

$$V_{ju2}=(1.1f_t b_j h_j+0.05N+f_{yv}A_{svj})/0.85 \tag{13}$$

$$b_j = \begin{cases} b_c & if \quad b_b \geq 0.5b_c \\ \min(b_b + 0.5h_c, b_c) & if \quad b_b < 0.5b_c \end{cases} \tag{14}$$

where f_c' and f_t are the compressive and tensile strengths of concrete, respectively. b_j is the effective joint width calculated by Eq. (14). b_b and b_c are the widths of beam and column sections, respectively. h_j is the joint section height and is equal to the column section height h_c. N is the column axial force. f_{yv} and A_{svj} are the yielding strength and sectional area of stirrups within joint core, respectively.

5.4 Prediction of failure modes and loading capacities

The failure modes of the BCJ specimens include beam failure with plastic hinge relocation, beam failure without plastic hinge relocation and joint shear failure. Figure 19 shows the procedure to predict the failure mode of BCJ specimens. The flexural capacities of beam sections without or with the anchorage segments (i.e. M_{bu0} and M_{bu}) and joint shear strength V_{ju} have to be first determined. Afterwards, the applied bending moment at the beam-joint interface M_{bj} needs to be calculated based on M_{bu0} and the anchorage length L_a as in Eq. (4), followed with a check on achievement of plastic hinge relocation by Eq. (5). Regardless of the achievement of plastic hinge relocation, the input shear force V_j can be estimated by Eq. (10) and is compared with the joint shear strength V_{ju}. If V_j is higher than V_{ju}, the failure mode of BCJs is determined as joint shear. Otherwise, it is judged as beam flexural failure with or without plastic hinge relocation.

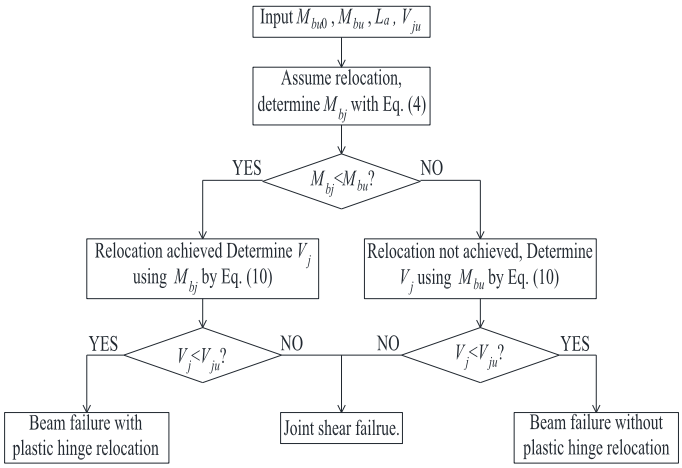

Figure 19: Flow chart to predict failure mode of BCJ specimens. [14]

For each failure mode, the corresponding loading capacity (horizontal load on column upper tip) can be calculated. For BCJs failed with relocated plastic hinges on beams, the applied bending moments on the plastic hinge sections reach the flexural capacity M_{bu0} of the beam section without the anchorage segments. The beam shear force V_b can be computed by Eq. (3).

The corresponding loading capacity P_u can be subsequently computed based on force equilibrium as Eq. (15).

$$P_u=2V_b(L_b+0.5h_c)/H_c \tag{15}$$

where H_c is the distance between inflection points on column, and h_c is the column section height.

For BCJs failed without plastic hinge relocation on beams (plastic hinges at the beam-joint interfaces), the shear force on the beam V_b can be determined by Eq. (16).

$$V_b=M_{bu}/L_b \tag{16}$$

where M_{bu} is the flexural capacity of beam with enhancement of the anchorage segments, and L_b is the distance beam inflection point to the beam-joint interface. Afterwards, the loading capacity corresponding to this failure mode P_u can be determined by Eq. (15).

For BCJs failed with joint shear, the input shear force V_j calculated by Eq. (10) exceeds the shear strength V_{ju} determined by Eqs. (11)-(14). In this situation the loading capacity of specimen is controlled by V_{ju}. The corresponding bending moment applied at the beam-joint interface M_{bj} can be estimated by sectional analysis with iterative calculations. Subsequently, the shear force on the beam V_b can be obtained with Eq. (17), and the loading capacity corresponding to this failure mode can be also determined by Eq. (15).

$$V_b=M_{bj}/L_b \tag{17}$$

5.5 Comparison of predicted and tested results

Table 3 summarizes the predicted and tested failue modes and loading capacities of BCJ specimens. The flexural capacities of beam sections M_{bu0} and M_{bu} are almost the same among the BCJ specimens as the same beam longitudinal reinforcement and concrete with a comparable strength were adopted. If the plastic hinges are assumed to be relocated, the applied

bending moment M_{bj} at the beam-joint interfaces increases with the longer anchorage length. The calculated M_{bu} of specimens J-0.25h_b, J-0.5h_b and J-0.75h_b is still higher than M_{bj}, meaning that the plastic hinges can be relocated. However, M_{bj} of specimen J-1.0h_b is higher than M_{bu}, indicating that plastic hinges cannot be relocated. Generally, the proposed analytical model is able to predict the achievement of plastic hinge relocation.

For BCJ specimens with $L_a \leqslant 0.75h_b$, the joint shear strength V_{ju} is higher than the joint shear force V_j (i.e. $V_{ju}/V_j>1$), indicating that the specimens fail by beam flexure rather than joint shear. Differently, V_{ju} of specimen J-1.0h_b is below its V_j (i.e. $V_{ju}/V_j<1$), and this specimen is regarded to fail by joint shear. As L_a increases from $0.75h_b$ to $1.0h_b$, the applied bending moments at the beam-joint interfaces are amplified, which subsequently increases the forces acting on the beam longitudinal reinforcement, anchorage segments and concrete. Although the forces on anchorage segments can be balanced, the increased forces on beam longitudinal reinforcement and concrete induce a higher joint shear force that surpasses the shear strength of BCJ. This prediction agrees well with the failure modes of the specimens in the test. It is worth noting that the joint shear strength V_{ju} decays under cyclic loading [32]. Therefore, V_{ju} of specimen J-1.0h_b failed in joint shear after beam yielding could be slightly higher than its V_j. Nevertheless, the joint shear strength V_{ju} estimated by the equations given in the code GB50010 [5] tends to be conservative. Thus, the model can still predict the occurrence of joint shear failure based on the ratio of V_{ju}/V_j.

The loading capacities of BCJ specimens can be subsequently predicted with the consideration of their failure modes. As seen in Table 3, a good agreement between predicted and tested results is obtained for all specimens. For instance, the loading capacity of specimen J-0.75h_b is overestimated by 8%, which is the highest overestimation among the BCJ specimens. This is probably caused by that the analytical model assuming that the plastic hinges in BCJs form exactly at the ends of the anchorage segments. However, the plastic hinges observed in the BCJ

specimens are distributed around the ends of the anchorage segments. It should also be noted that for specimen J-1.0h_b, its estimated loading capacity also agrees with the prediction. Therefore, the proposed analytical model is able to predict the loading capacities of the BCJ specimens failed by both beam plastic hinges and joint shear.

Table 3: Predicted and tested failure modes and loading capacities of specimens

Specimen	Prediction								Test		$P_{u,pred}/P_{u,test}$
	M_{bu0}	M_{bj}	M_{bu}	V_j	V_{ju}	V_{ju}/V_j	Failure mode	$P_{u,pred}$	Failure mode	$P_{u,test}$	
JC	61.4	N/A	N/A	394.6	599.3	1.51	B	65.9	B	69.6	0.95
J-0.25h_b	61.8	67.6	89.6	355.8	458.0	1.29	BR	72.6	BR	70.4	1.03
J-0.5h_b	61.6	73.9	89.4	381.2	447.6	1.17	BR	79.4	BR	78.3	1.01
J-0.75h_b	61.1	81.2	88.8	385.2	421.5	1.09	BR	86.3	BR	79.8	1.08
J-1.0h_b	61.6	92.5	89.4	466.8	449.7	0.96	J	89.9	BJ	88.7	1.01
B: beam failure without plastic hinge relocation; BR: beam failure with plastic hinge relocation; J: joint shear failure. BJ: beam failure followed by joint shear failure.											

6. Conclusions

This paper investigated the seismic performance of RC interior BCJs reinforced with the unbonded diagonal bars mechanically anchored in beams. The influence of the relocating distance for plastic hinges on the seismic performance of BCJs and the effectiveness of the proposed reinforcement detail were studied. Moreover, an analytical model was also developed for predicting the failure modes and loading capacities of BCJs. Based on the results and discussion, the following conclusions can be made.

(1) The use of mechanically anchored diagonal bars can successfully relocate the plastic hinges from the beam-joint interfaces to the end of anchorage segments by a distance between 0.25h_b and 0.75h_b. However, the applied bending moments at the beam-joint interfaces are amplified with the plastic hinges relocated farther away, and increasing the

anchorage length to $1.0h_b$ results in unsuccessful plastic hinge relocation and triggers joint shear failure.

(2) The increase of relocating distance from $0.25h_b$ to $1.0h_b$ enhances the loading capacity of BCJ specimens. However, this improvement is restrained by joint shear strength as the farther relocation of plastic hinges further increases the joint shear demand. The impact of the relocating distance for plastic hinge on the ductility, energy dissipation, stiffness is limited. Moreover, the joint shear deformation of BCJs first decreases and then increases with the relocating distance.

(3) The adoption of a longer relocating distance for plastic hinge can reduce the yielding penetration of beam longitudinal reinforcement into joint core. Meanwhile, increasing the anchorage length enhances the effectiveness of the anchorage segments in increasing flexural resistance at the beam-joint interface. Consequently, the forces balanced on the diagonal segments increase so that the strength of the diagonal segments can be further utilized.

(4) The relocating distance for plastic hinge in BCJs should be longer than the code-specified development length of anchorage segments to ensure their stress developmentand reduce yielding penetration of beam longitudinal reinforcement. Meanwhile, the distance should also be controlled whthin $0.75h_b$ to achieve plastic hinge relocation and prevent joint shear failure.

(5) An analytical model considering plastic hinge relocation and force self-balancing mechanisms is proposed for BCJs with the novel reinforcement detail. The model can successfully predict the achievement of plastic hinge relocation, joint shear failure and loading capacities of BCJ specimens. Therefore, the model can be used to guide the selection of the relocating distance for plastic hinge in BCJs.

Acknowledgement

The authors wish to acknowledge the financial support of National Natural Science Foundation of China (No.: 51708306), Zhejiang Provincial Key R&D Programme (No.: 2021C03162), and Ningbo Municipal Bureau of Science and Technology (No.: 2019B10048 and 2019C50017). The Zhejiang Provincial Department of Science and Technology is also acknowledged for this research under its Provincial Key Laboratory Programme (No.: 2020E10018).

References

[1] Paulay T, Priestley MJN. Seismic Design of Reinforced Concrete and Masonry Buildings. 1992.

[2] Walker SG. Seismic Performance of Existing Reinforced Concrete Beam-Column Joints. MSc Thesis, University of Washington, 2001.

[3] Tapan M, Comert M, Demir C, Sayan Y, Orakcal K, Ilki A. Failures of structures during the October 23, 2011 Tabanlı (Van) and November 9, 2011 Edremit (Van) earthquakes in Turkey. Eng Fail Anal 2013;34:606–28.

[4] Sezen H, Whittaker AS, Elwood KJ, Mosalam KM. Performance of reinforced concrete buildings during the August 17, 1999 Kocaeli, Turkey earthquake, and seismic design and construction practise in Turkey. Eng Struct 2003;25:103–14.

[5] China Building Industry Press. Code for design of concrete structures. GB50010. 2015th ed. Beijing: China Building Industry Press; 2015.

[6] ACI 318-02. Building code requirements for structural concrete and commentary. Detroit, Michigan: 2002.

[7] NZS3101-1. Concrete structures standard - The design of concrete structures. 2006.

[8] Bai J, Ou J. Realization of the global yield mechanism of RC frame structures by redesigning the columns using column tree method. Sci China Technol Sci 2015;58:1627–37.

[9] Palissery S, Murty CVR, Goswami R. Quantifying Parameters that ensure Large Deformability of Earthquake Resistant RC Buildings in High Seismic Regions. 2014.

[10] Elmenshawi A, Brown T, El-Metwally S. Plastic hinge length considering shear reversal in reinforced concrete elements. J Earthq Eng 2012;16:188–210.

[11] Yang H, Zhao W, Zhu Z, Fu J. Seismic behavior comparison of reinforced concrete interior beam-column joints based on different loading methods. Eng Struct 2018;166:31–45.

[12] Engindeniz M, Kahn LF, Zureick AH. Repair and strengthening of reinforced concrete beam-column joints: State of the art. ACI Struct J 2005;102:187–97.

[13] Zhang X, Li B. Seismic Performance of RC Beam–Column Joints Constructed with Engineered Cementitious Composites. J Struct Eng 2020;146:04020271.

[14] Shen X, Li B, Chen Y-T, Tizani W. Seismic performance of reinforced concrete interior beam-column joints with novel reinforcement detail. Eng Struct 2021;227:111408.

[15] Park R, Milburn JR. Comparison of recent New Zealand and United States seismic design provisions for reinforced concrete beam-column joints and test results from four units designed according to the New Zealand code. Bull New Zeal Natl Soc Earthq Eng 1983;16:3–24.

[16] Sharif MR, Ketabi MS. An improved plastic hinge relocation technique for RC beam–column joints: experimental and numerical investigations. Bull Earthq Eng 2020;18:4191–225.

[17] Hwang H-J, Eom T-S, Park H-G. Design considerations for interior RC beam-column joint with additional bars. Eng Struct 2015;98:1–13.

[18] Chutarat N, Aboutaha RS. Cyclic response of exterior reinforced concrete beam-column joints reinforced with headed bars - Experimental investigation. ACI Struct J 2003;100:259–64.

[19] Galunic B, Bertero VV, Popov EP. An approach for improving seismic behavior of reinforced concrete interior joints. vol. 77. College of Engineering, University of California; 1977.

[20] Eom T-S, Park H-G, Hwang H-J, Kang S-M. Plastic Hinge Relocation Methods for Emulative PC Beam–Column Connections. J Struct Eng 2016;142:04015111.

[21] Eslami A, Ronagh HR. Experimental investigation of an appropriate anchorage system for flange-bonded carbon fiber-reinforced polymers in retrofitted RC beam-column joints. J Compos Constr 2014;18:1–11.

[22] Mostofinejad D, Akhlaghi A. Experimental Investigation of the Efficacy of EBROG Method in Seismic Rehabilitation of Deficient Reinforced Concrete Beam–Column Joints Using CFRP Sheets. J Compos Constr 2017;21:04016116.

[23] Ilia E, Mostofinejad D. Seismic retrofit of reinforced concrete strong beam–weak column joints using EBROG method combined with CFRP anchorage system. Eng Struct 2019;194:300–19.

[24] Wang G, Dai J, Bai Y. Seismic retrofit of exterior RC beam-column joints with bonded CFRP reinforcement: An experimental study. Compos Struct 2019;224:111018.

[25] Shafaei J, Hosseini A, Marefat MS. Seismic retrofit of external RC beam-column joints by joint enlargement using prestressed steel angles. Eng Struct 2014;81:265–88.

[26] Shafaei J, Nezami SA. Effect of different size of joint enlargement on seismic behavior of gravity load designed RC beam-column connections. Struct Des Tall Spec Build 2019;28:1–27.

[27] Maddah A, Golafshar A, Saghafi MH. 3D RC beam–column joints retrofitted by joint enlargement using steel angles and post-tensioned bolts. Eng Struct 2020;220:110975.

[28] Arowojolu O, Ibrahim A, Rahman MK, Al-Osta M, Al-Gadhib AH. Plastic hinge relocation in reinforced concrete beam–column joint using carbon fiber–reinforced polymer. Adv Struct Eng 2019;22:2951–65.

[29] Lu X, Urukap TH, Li S, Lin F. Seismic behavior of interior RC beam-column joints with additional bars under cyclic loading. Earthq Struct 2012;3:37–57.

[30] BS EN 206:2013. Concrete - Specification , performance , production and conformity. 2013.

[31] Li B, Lam ESS, Wu B, Wang YY. Experimental investigation on reinforced concrete interior beam-column joints rehabilitated by ferrocement jackets. Eng Struct 2013;56:897–909.

[32] Shin M, LaFave JM. Modeling of cyclic joint shear deformation contributions in RC beam-column connections to overall frame behavior. Struct Eng Mech 2004;18:645–69.